

Summary of ERB Recommended Study – Items 3.2 and 3.3

Do Jun Shim*
Engineering Mechanics Corporation of Columbus (Emc²)

February 4, 2016

1. Introduction

The External Review Board (ERB) for xLPR has raised questions regarding the possibility of non-LBB conditions for several scenarios of crack growth. The meeting was held in Washington D.C. on October 29-30, 2014 and recommendations were made in a report that was sent on December 3, 2014. There are essentially two areas of concern that need to be addressed regarding this issue.

The first is with regard to the effect of weld residual stresses (WRS) on circumferential through-wall crack growth. Consider an axial WRS field that has high values of compression near the mid thickness region. As a PWSCC crack is growing through the thickness, the growth in the depth direction will slow down when this compressive WRS field is reached, especially if the service bending loads are relatively small. However, near the crack tips the crack may continue to grow circumferentially, possibly approaching a 360-degree crack prior to leakage. This may lead to a non-LBB situation that the xLPR code needs to address. The actual comments by ERB are shown in Figure 1.

The second area of study recommended by the ERB is with regard to the effect of WRS fields on TWC crack growth, specifically its effect on crack opening displacement (COD) and therefore leak rate. The ERB comments and recommendations are shown in Figure 2.

This document summarizes the efforts taken to address the ERB comments. Descriptions and results of analyses performed are provided in this document along with the conclusions obtained from these efforts. Note that these analyses were not part of the original xLPR workscope, and were conducted to satisfy the ERB questions. If the conclusions of this study raise additional issues, a more comprehensive study would be needed.

2. Description of Analyses and Results

In this effort, various analyses were performed to address the two comments (Item 3.2 and Item 3.3) provided by the ERB. First, as recommend by the ERB, advanced finite element analyses (AFEAs) were performed for typical surge nozzle and hot-leg nozzle geometries. For both cases, PWSCC in dissimilar metal (DM) welds was assumed. From these analyses, the natural crack growth behavior of a PWSCC in a DM weld under normal operating conditions (with relatively low global bending stress) and WRS was evaluated. All analyses started with an initial surface

* Currently at Structural Integrity Associates, Inc. (dshim@structint.com)

crack that propagated to penetrate the pipe wall to form a transition crack that eventually formed an idealized through-wall crack. In some cases the WRS was removed for the through-wall crack growth portion to investigate the effect of WRS on through-wall crack growth. After the AFEA calculations were completed, the crack growth behavior was predicted using the xLPR Ver. 2.0 Code. This was done to see if the xLPR code can predict the relatively long surface crack that is formed prior to wall penetration in the AFEA. Based on the reasonable agreement between the AFEA and xLPR results, the stability and leak rate calculations were conducted using the xLPR code with some additional input such as safe-shutdown earthquake (SSE) loads. These results were then used to investigate the LBB behavior.

3.2 An evaluation should be made on the possibility that a surface crack grows to have a very long circumferential length (or even to a fully circumferential crack) before it penetrates the pipe wall. After wall penetration, the crack length and COD along the OD may be so small that it is not discovered by leak-rate detection before the continuing crack growth leads to pipe rupture. This non-LBB situation, which is not generally covered by xLPR, can occur for a weld residual stress field (WRS) that has compressive stresses in the middle of the pipe wall in combination with very small operating stresses from global bending. Based on preliminary calculations performed by the ERB, the following parameter combination is proposed for study using advanced finite element analysis (AFEA):

a) A typical surge nozzle geometry ($D_0 = 381$ mm, $t = 40.1$ mm) with a WRS taken from supplement Q25 (slide 3) in the Replies to xLPR ERB comments from February 2013, "Effects of WRS on TWC Growth - Results from limited case studies" by Do-Jun Shim. This WRS should be combined with global bending stresses of the range 0 - 20 MPa. Internal pressure is 15.4 MPa. A proposed initial crack size with subsequent crack growth is a depth = 1 mm, and length = 5-10 % of the pipe circumference.

b) A typical hot-leg nozzle geometry ($D_0 = 862$ mm, $t = 60.2$ mm) with a WRS taken from supplement Q25 (slide 7). This WRS should be combined with global bending stresses in the range 0 - 20 MPa. Internal pressure is 15.4 MPa. A proposed initial crack size for subsequent crack growth is a depth = 1 mm, length = 5-10 % of the pipe circumference.

If the existence of such non-LBB situations is verified by AFEA, the xLPR team should identify the level of global bending stresses in combination with typical WRS that can cause this situation and determine if pipes in plants subjected to PWSCC can experience this during operation.

Figure 1 ERB comments on LBB

3.3 The xLPR code ignores WRS for PWSCC growth of a through-wall crack (TWC) and also for COD and leak-rate evaluation. This is probably a justified assumption in most cases. However, for a combination of WRS and small operating stresses from global bending that cause very long circumferential cracks before wall penetration, the effect of WRS on TWC can be important. The WRS may cause crack growth on the OD to propagate relatively slowly up to the point of pipe rupture. A non-idealized crack shape will thus be present at rupture causing a smaller leak rate compared to the situation if WRS is ignored. In analogy with item 3.2, this effect is seen only when the operating stresses from global bending are low. In contrast, a large global bending stress will (almost) totally extinguish the effect of WRS causing a straight crack front (parallel to the pipe radius) before rupture is predicted.

The ERB recommends that the xLPR team employ advanced finite element analysis (AFEA) to study the effect of WRS on TWC (regarding crack growth, COD and leak rate) using the same parameter combination of WRS and global bending stresses as in item 3.2. Note: for a particular TWC geometry (also for a non-idealized crack shape), the effect of WRS on leak rate is not significant. But since WRS will affect crack growth for a TWC if the global bending stress is small, WRS will also indirectly influence the COD and leak rate just before rupture. The problem is also related to the stability criterion used. The effect of WRS on TWC growth becomes more pronounced when the stability is controlled by J (which accounts for the secondary WRS stresses) compared to application of net section collapse criterion.

If the influence of WRS on TWC behavior is verified by AFEA, the xLPR team should identify the level of global bending stresses in combination with typical WRS that can cause this situation to develop and determine if pipes in plants subjected to PWSCC can experience this during operation.

Figure 2 ERB comments on effect of WRS on TWC growth, COD and leak rate

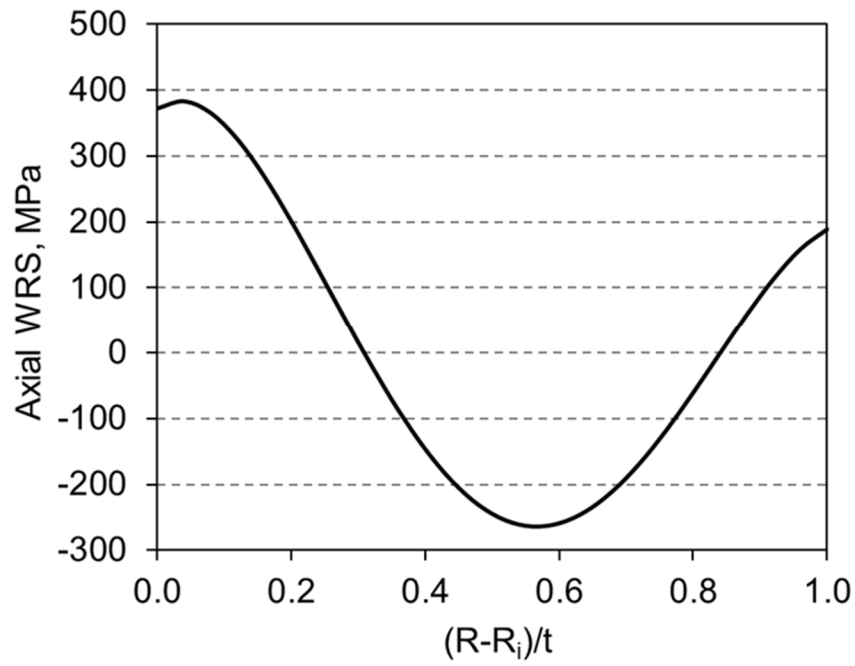
2.1 AFEA matrix

Table 1 provides the original AFEA matrix that was proposed for this effort. However, as described later in this report, all cases were not needed to address the comments provided by the ERB. Table 1 provides the pipe/nozzle geometry, normal operating conditions, and the initial PWSCC size for each case based on ERB's suggestions (see Figure 1). The internal pressure and axial tension values were fixed at 15.4 MPa and 27.6 MPa, respectively. The global bending stress value varied from 0 to 20 MPa. The initial crack depth (a) was selected as 10 percent of the wall thickness (t) or $a/t=0.1$. The initial surface crack length was 5 percent of the pipe circumference. The normal operating temperature was assumed as 340C and the corresponding PWSCC crack growth rate for Alloy 182 (75th percentile) was determined from MRP-115. Figure 3 depicts the axial WRS profiles used for the AFEA calculations (these profiles are the ones that are mentioned in Figure 1). Note that in AFEA, normal operating loads and WRS are applied to an elastic FE model. The elastic material properties used in the analyses were $E=195,100$ MPa and $\nu=0.3$.

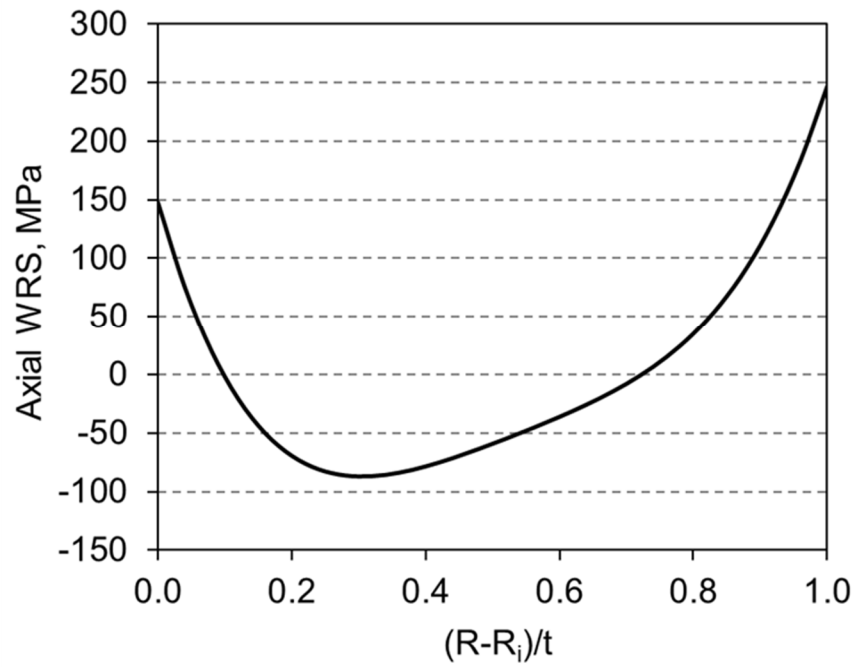
Table 1 Proposed analysis matrix for ERB recommended study

Case ID	Do mm	t mm	Pressure MPa	Tension* MPa	Bending MPa	Axial WRS	a,init mm	c _{inner} ,init mm	a/t	a/c _{inner}
SN1	381	40.1	15.4	27.6	0	YES	4	23.6248	0.10	0.169
SN2	381	40.1	15.4	27.6	20	YES	4	23.6248	0.10	0.169
SN2-1	381	40.1	15.4	27.6	20	SC:YES TWC:NO	4	23.6248	0.10	0.169
SN3	381	40.1	15.4	27.6	0	NO	4	23.6248	0.10	0.169
SN4	381	40.1	15.4	27.6	20	NO	4	23.6248	0.10	0.169
HL1	862	60.2	15.4	27.6	0	YES	6	58.2451	0.10	0.103
HL2	862	60.2	15.4	27.6	20	YES	6	58.2451	0.10	0.103
HL2-1	862	60.2	15.4	27.6	20	SC:YES TWC:NO	6	58.2451	0.10	0.103
HL3	862	60.2	15.4	27.6	0	NO	6	58.2451	0.10	0.103
HL4	862	60.2	15.4	27.6	20	NO	6	58.2451	0.10	0.103

* Including tension due to internal pressure



(a) Surge nozzle



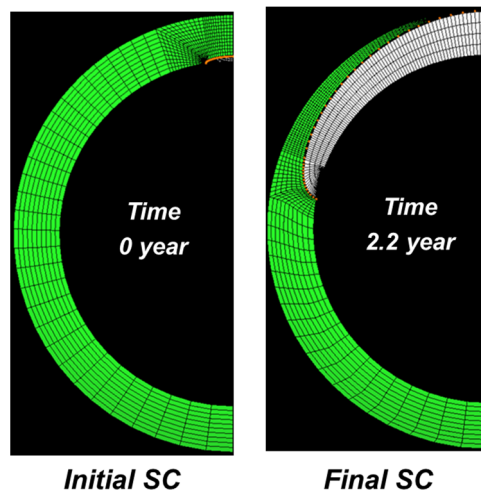
(b) Hot-leg nozzle

Figure 3 Axial WRS profiles used in AFEA for (a) surge nozzle and (b) hot-leg nozzle

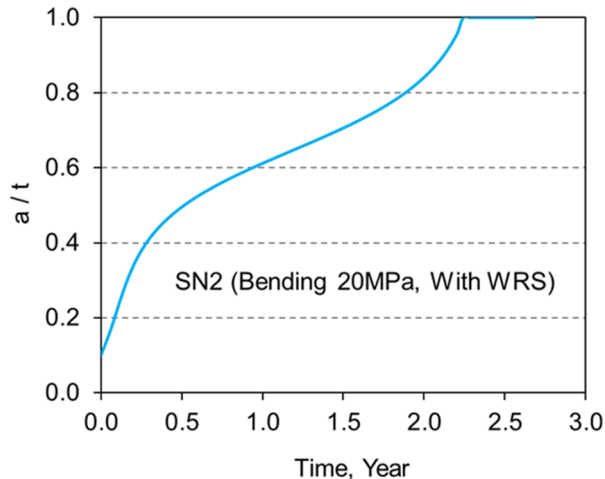
2.2 AFEA results

Surge nozzle results

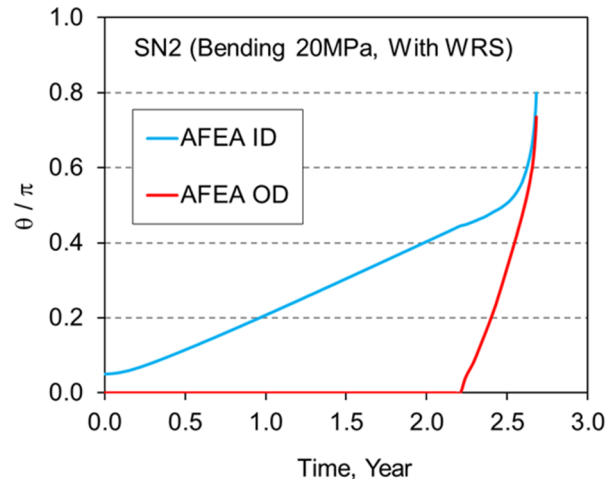
Figure 4 provides the AFEA results for the surge nozzle case (SN2) with 20 MPa global bending and axial WRS applied for both surface crack and through-wall crack growth. The initial and final surface crack shapes are shown in Figure 4(a). Due to the relatively low global bending stress and the compressive axial WRS at mid-wall thickness, the final surface crack length prior to wall penetration was approximately 45% of the pipe circumference. Figure 4(b) depicts the surface crack growth in the thickness direction as a function of time. In addition, the crack growth in the circumferential direction is provided in Figure 4(c). As shown in this figure, after wall penetration, a non-idealized through-wall crack is formed where the crack length on the OD surface is much smaller than that at the ID surface. However, the non-idealized through-wall crack quickly transitions to an idealized through-wall crack.



(a) Initial and final surface crack shapes



(b) Crack growth in the thickness direction

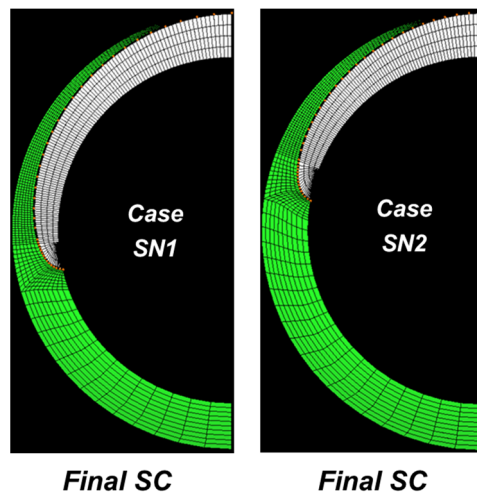


(c) Crack growth in the circumferential direction

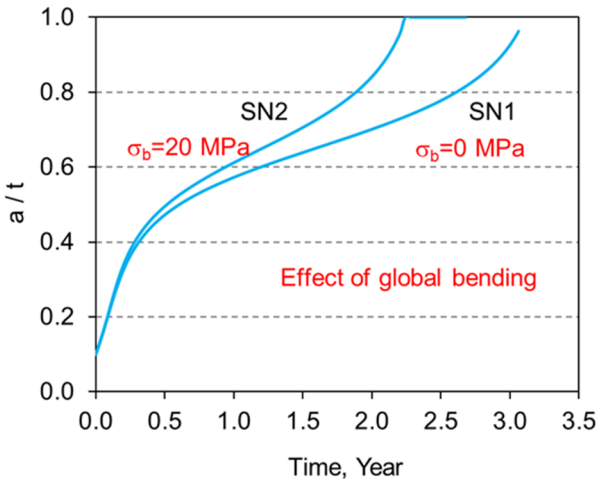
Figure 4 AFEA results for Case SN2 (surge nozzle)

In order to investigate the effect of global bending on crack growth behavior, AFEA results from Case SN2 were compared with those from Case SN1 where no global bending was applied (other inputs remained the same). Figure 5(a) compares the final surface crack shapes from the two cases. The surface crack growth in the circumferential direction was larger for Case SN1 – 57% of the circumference at wall penetration. In addition, as expected, the time to wall penetration was higher for Case SN1 compared to Case SN2, see Figure 5(b). Due to meshing limitations, the through-wall crack growth for Case SN1 was not performed.

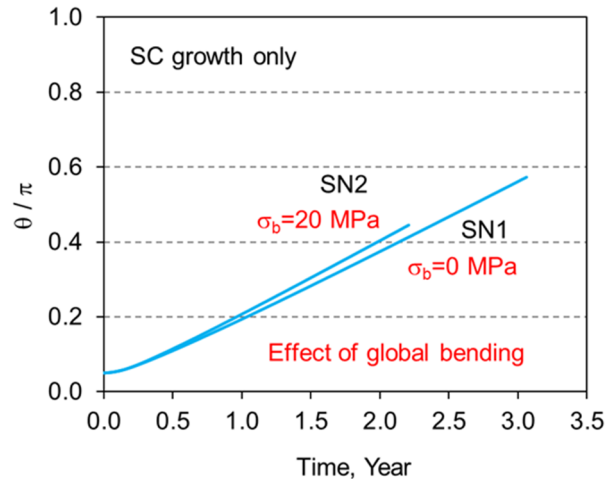
The effect of axial WRS on surface crack growth is shown in Figure 6. As demonstrated in this figure, the final surface crack shape is mainly driven by the WRS. The relatively long surface crack (SN2) is not formed without the WRS as shown for Case SN4. Hence, Case SN4 is not a concern for the ERB scenario and based on this result AFEA for Case SN3 was not conducted.



(a) Comparison of final surface crack shapes

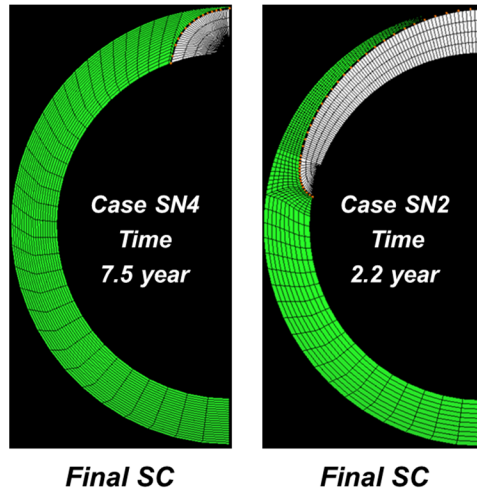


(b) Crack growth in the thickness direction

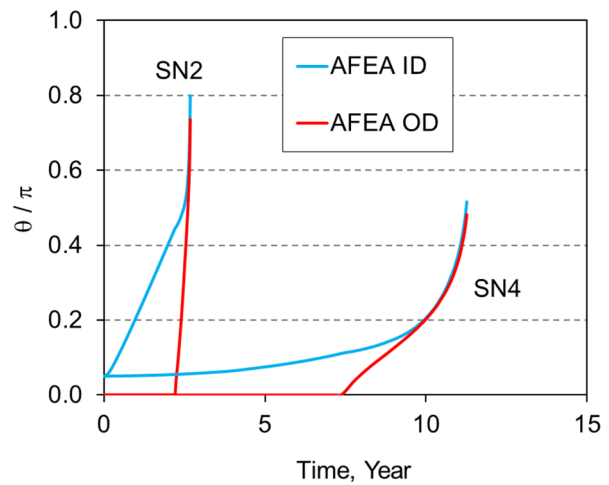
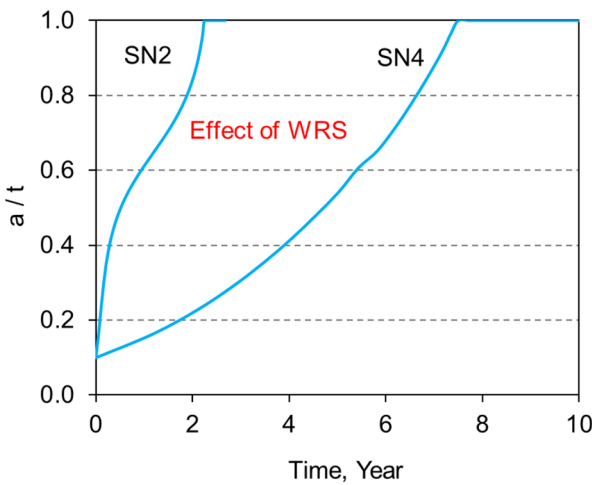


(c) Crack growth in the circumferential direction

Figure 5 Effect of global bending on AFEA results (surge nozzle)



(a) Comparison of final surface crack shapes



(b) Crack growth in the thickness direction

(c) Crack growth in the circumferential direction

Figure 6 Effect of WRS on AFEA results (surge nozzle)

One of the main concerns that the ERB expressed was the effect of WRS on through-wall crack growth. To investigate this effect, the through-wall crack growth portion of Case SN2 was reanalyzed without the WRS in the AFEA calculations. The results are provided in Figure 7 where Case SN2-1 represents the through-wall crack growth without the WRS. Figure 7(b) compares the through-wall crack growth behavior after wall penetration. For this particular case, the effect of WRS on through-wall crack growth is very small. Closer observations indicate that the crack growth rate on the ID surface reduces and that on the OD surface increases when the WRS is removed. It will be shown later in this report that this difference has no effect on the LBB analysis results.

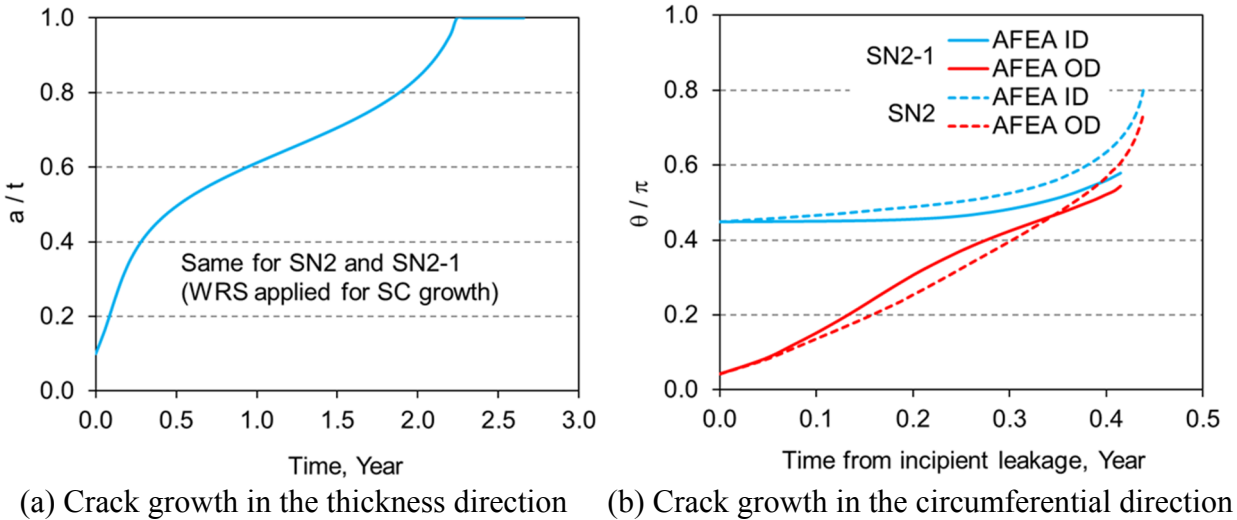


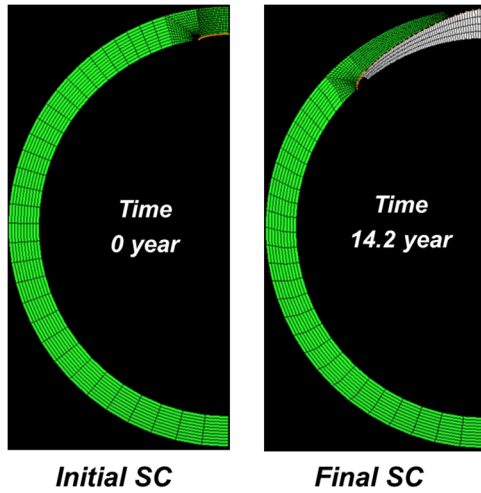
Figure 7 Effect of WRS on through-wall crack growth (surge nozzle)

Hot-leg nozzle results

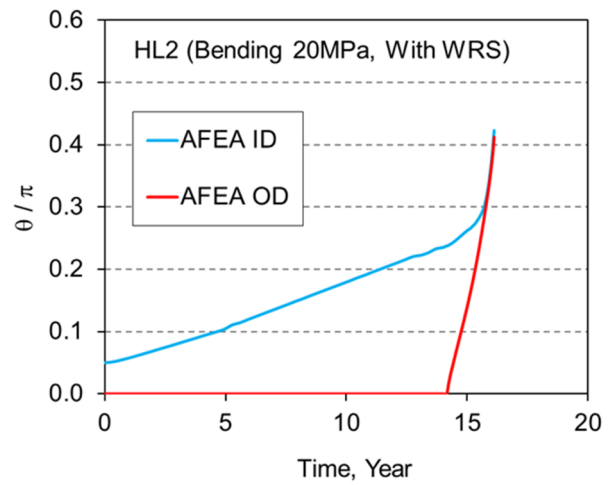
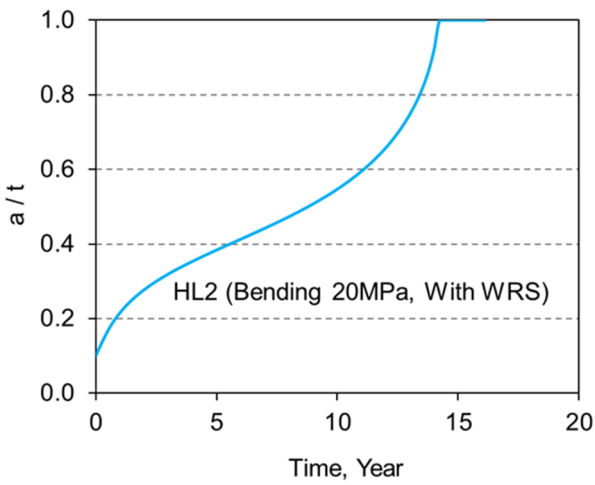
Figure 8 provides the AFEA results for the hot-leg nozzle case (HL2) with 20 MPa global bending and axial WRS applied for both surface crack and through-wall crack growth. The initial and final surface crack shapes are shown in Figure 8(a). Here again, due to the relatively low global bending stress and the compressive axial WRS around mid-wall thickness, the final surface crack length was approximately 24% of the pipe circumference prior to wall penetration. The crack growths in the thickness direction and the circumferential direction are provided in Figure 8(b) and Figure 8(c), respectively. Similar to the surge nozzle case, the non-idealized through-wall crack rapidly transitions to an idealized through-wall crack. Based on the results from the surge nozzle (where global bending of 20 MPa did not significantly affect the surface crack length prior to wall penetration), the AFEA cases with no global bending stress were not performed for the hot-leg nozzle (Case HL1 and Case HL3 in Table 1).

The effect of axial WRS on surface crack growth is shown in Figure 9. Again, it is demonstrated that the final shape of the surface crack is strongly driven by the WRS. For the relatively short surface crack formed in Case HL4, there is no major concern with the xLPR predictions for LBB.

Similar to the surge nozzle case, the effect of WRS on through-wall crack growth was investigated for the hot-leg nozzle case as shown in Figure 10. The cases with WRS (HL2) and without WRS (HL2-1) for through-wall crack growth are compared in Figure 10(b). For this specific comparison, the crack growth rate on the OD surface increased when the WRS was removed whereas there was not much difference in the ID crack growth rate until it formed an idealized through-wall crack. However, as shown later in this report, this difference does not have a significant effect on the LBB predictions.

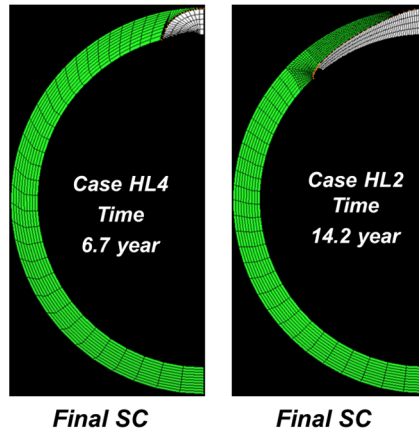


(a) Initial and final surface crack shapes

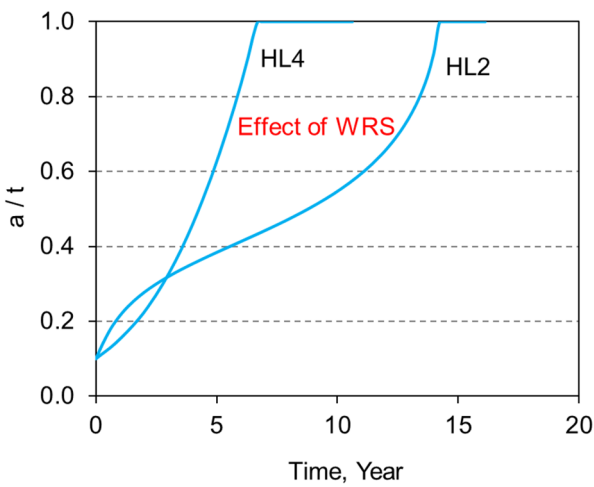


(b) Crack growth in the thickness direction (c) Crack growth in the circumferential direction

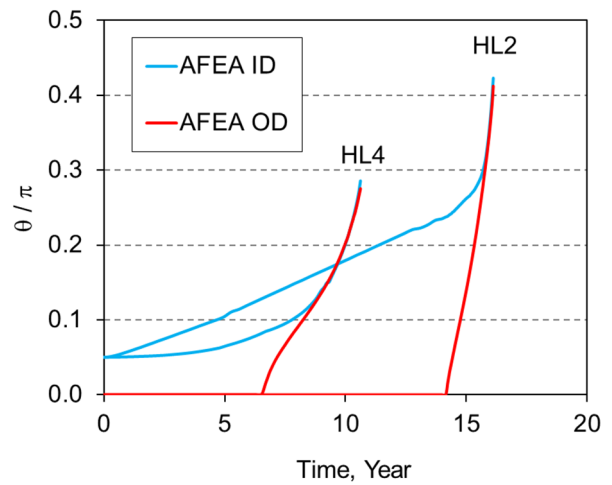
Figure 8 AFEA results for Case HL2 (hot-leg nozzle)



(a) Comparison of final surface crack shapes

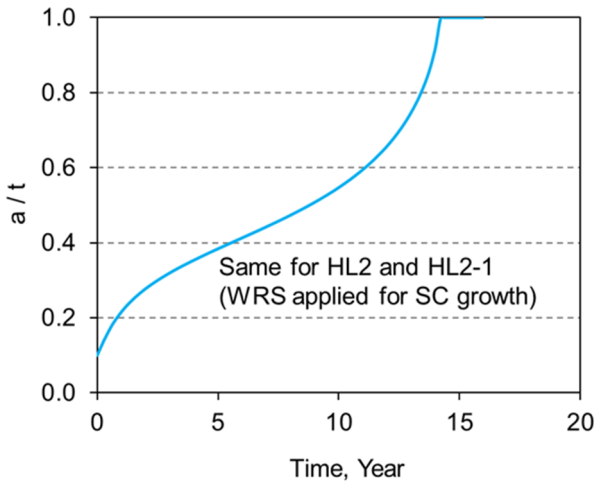


(b) Crack growth in the thickness direction

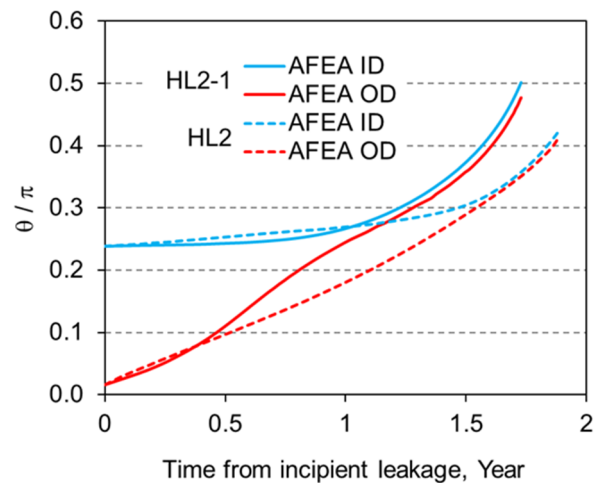


(c) Crack growth in the circumferential direction

Figure 9 Effect of WRS on AFEA results (hot-leg nozzle)



(a) Crack growth in the thickness direction



(b) Crack growth in the circumferential direction

Figure 10 Effect of WRS on through-wall crack growth (hot-leg nozzle)

2.3 Comparison with xLPR results

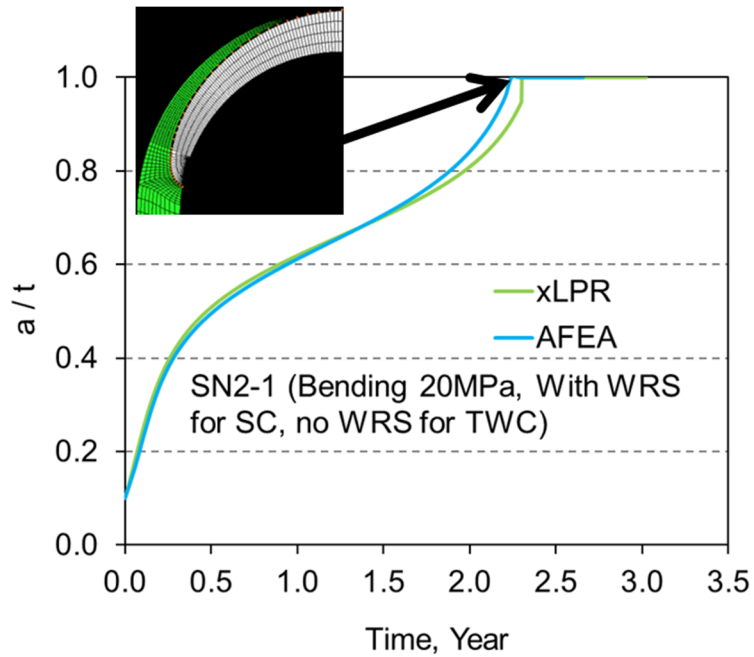
Using the same input from the AFEA, PWSCC crack growth was predicted using the xLPR Ver. 2.0 code. Note that in the current version of xLPR, the WRS is neglected for the through-wall crack growth. Hence, AFEA results without WRS for through-wall crack (i.e., SN2-1 and HL2-1) were used for comparisons.

Figure 11 provides comparisons between xLPR and AFEA results for the surge nozzle case. As shown in Figure 11(a), the crack growth in the depth direction showed good agreement up to wall penetration. In addition, the surface crack lengths at wall penetration were within 7% difference - see Figure 11(b). Note that in xLPR the surface crack is idealized as a semi-ellipse throughout the entire crack growth analysis whereas natural crack shape is formed in the AFEA. The two results showing good agreement indicates that the shape of the surface crack in the AFEA remained relatively close to a semi-ellipse as illustrated in the insert in Figure 11(a).

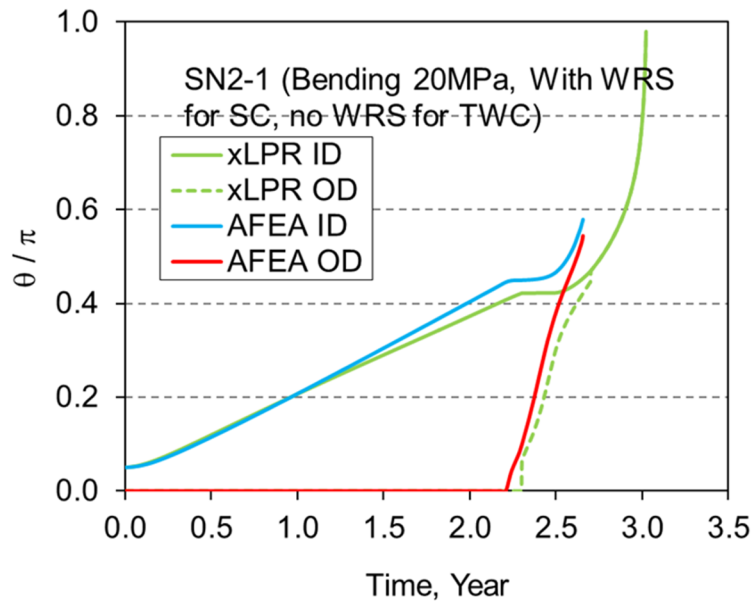
After wall penetration, the non-idealized through-wall crack growth is simulated by the crack transition model in xLPR. As provided in Figure 11(b), the crack transition to idealized through-wall crack is well captured by the xLPR code. The slight difference between the two results is mainly due to the difference in the ID surface crack lengths at wall penetration. The idealized through-wall crack growth was continued in the xLPR run since the stability module was not turned on for this comparison. Stability and leak rate calculation results are provided in the next subsection.

Similar comparisons for the hot-leg nozzle are shown in Figure 12. For this case, the surface crack growth results showed some difference – both in the depth and circumferential directions. This is due to the natural surface crack shape deviating from the semi-ellipse shape in the AFEA as illustrated in the insert in Figure 12(a). However, the trends of the crack transition and the idealized through-wall crack growth are very similar.

The results provided in Figure 11 (and Figure 7) and Figure 12 (and Figure 10) demonstrate that the LBB analyses (stability and leak rate calculations) can be investigated using the xLPR code.

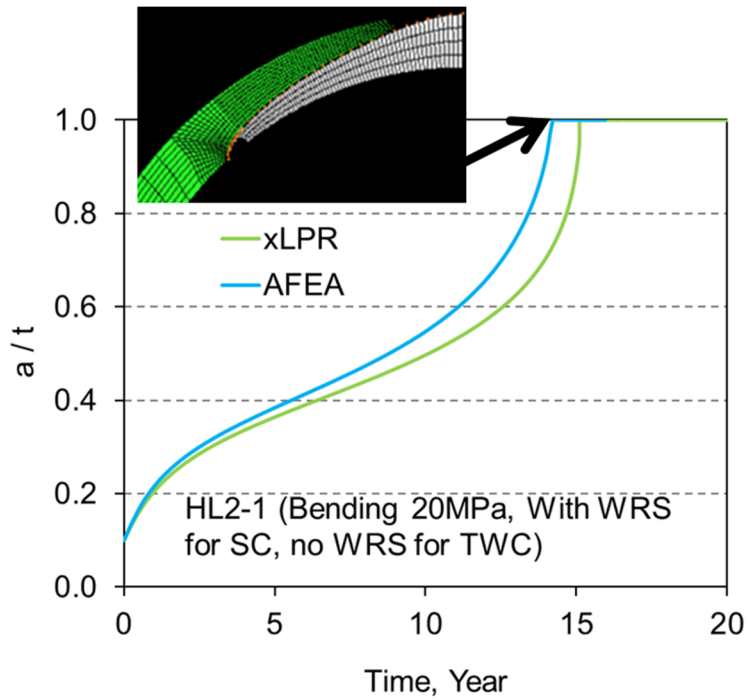


(a) Crack growth in the thickness direction

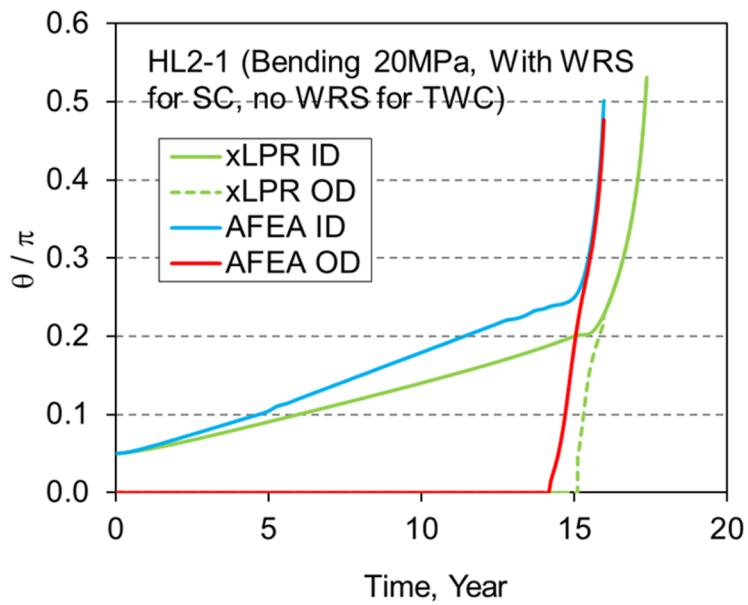


(b) Crack growth in the circumferential direction

Figure 11 Comparison of AFEA and xLPR (surge nozzle)



(a) Crack growth in the thickness direction



(b) Crack growth in the circumferential direction

Figure 12 Comparison of AFEA and xLPR (hot-leg nozzle)

2.4 Stability and leak rate calculations

The elastic-plastic material properties and the fracture toughness properties of the DM weld and base metal provided by the Inputs Group were used for the stability and leak rate calculations. Figure 13 summarizes the input data. For the present xLPR calculations, the DM weld mixture ratio (MR) was fixed to 0.5 which typically corresponds to a crack in the center of the DM weld.

The SSE loads for surge nozzle[†] and hot-leg nozzle[‡] are provided in Table 2. These loads were added to the normal operating loads for the stability calculations. For the leak rate calculations, only the normal operating loads were used.

■ SS 316 (left pipe)

General Properties (2301 - 2310)							
2301	Yield Strength, Sig _y	MPa	Constant	no	0.5	204	
2302	Ultimate Strength, Sig _u	MPa	Constant	no	0.5	462.7	
2303	Ramberg-Osgood Coef, F	MPa	Constant	no	0.5	649.2	
2304	Ramberg-Osgood Coef, n		Constant	no	0.5	4.84	
2305	Elastic Modulus, E	MPa	Constant	no	0.5	195100	
2306	Material Init J-Resistance, J _{ic}	N/mm	Constant	no	0.5	224.6	
2307	Material Init J-Resist Coef, C	N/mm	Constant	no	0.5	265	
2308	Material Init J-Resist Exponent, m		Constant	no	0.5	0.415	

■ SA 508 (right pipe)

General Properties (2101 - 2110)							
2101	Yield Strength, Sig _y	MPa	Constant	no	0.5	268	
2102	Ultimate Strength, Sig _u	MPa	Constant	no	0.5	620	
2103	Ramberg-Osgood Coef, F	MPa	Constant	no	0.5	926.7	
2104	Ramberg-Osgood Coef, n		Constant	no	0.5	4.24	
2105	Elastic Modulus, E	MPa	Constant	no	0.5	195100	
2106	Material Init J-Resistance, J _{ic}	N/mm	Constant	no	0.5	233.15	
2107	Material Init J-Resist Coef, C	N/mm	Constant	no	0.5	296.3	
2108	Material Init J-Resist Exponent, m		Constant	no	0.5	0.564	

■ Alloy 182 (weld)

General Properties (2501 - 2510)							
2501	Yield Strength, Sig _y	MPa	Constant	no	0.5	229.1283916	
2502	Ultimate Strength, Sig _u	MPa	Constant	no	0.5	560	
2503	Ramberg-Osgood Coef, F	MPa	Constant	no	0.5	600	
2504	Ramberg-Osgood Coef, n		Constant	no	0.5	4	
2505	Elastic Modulus, E	MPa	Constant	no	0.5	195100	
2506	Material Init J-Resistance, J _{ic}	N/mm	Constant	no	0.5	554.1772727	
2507	Material Init J-Resist Coef, C	N/mm	Constant	no	0.5	586.2801947	
2508	Material Init J-Resist Exponent, m		Constant	no	0.5	0.660865625	

Figure 13 Summary of elastic-plastic material properties and fracture toughness properties

Table 2 Summary of SSE loads

Case	Total axial tension stress, MPa	Total global bending stress, MPa
Surge nozzle	0.65	34.74
Hot-leg nozzle	23.24	100.68

[†] Extracted from xLPR Ver. 1 Pilot Study Report

[‡] Extracted from Westinghouse 4-Loop RPV Inlet-Outlet Nozzle Inputs (MCOE-LTR-12-63)

Figure 14 shows the xLPR stability calculation results for surge and hot-leg nozzles. As illustrated in this figure, for both cases, the critical crack size was obtained after the non-idealized through-wall crack fully transitioned to an idealized through-wall crack. Furthermore, the critical crack size was approximately 50% of the circumference for both cases. As described earlier, these results do not include the WRS for the through-wall crack stability calculations. However, results from past work[§] have demonstrated that the secondary stresses (WRS and thermal transient stress) are overwhelmed by the primary stresses as the crack approaches the critical crack size. Hence, the J-controlled stability method used in xLPR should not be an issue for typical cases.

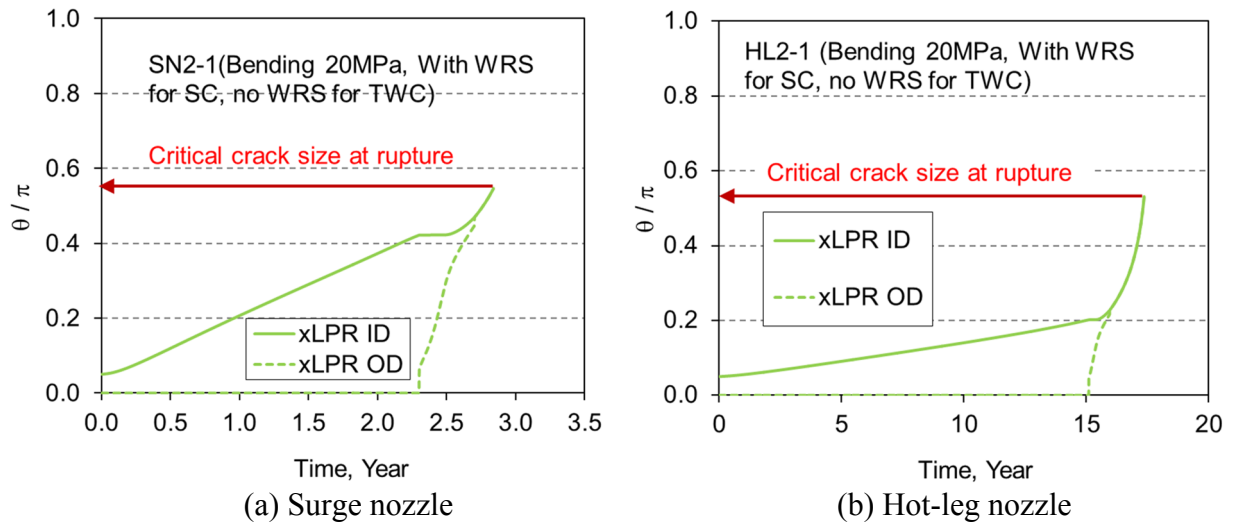


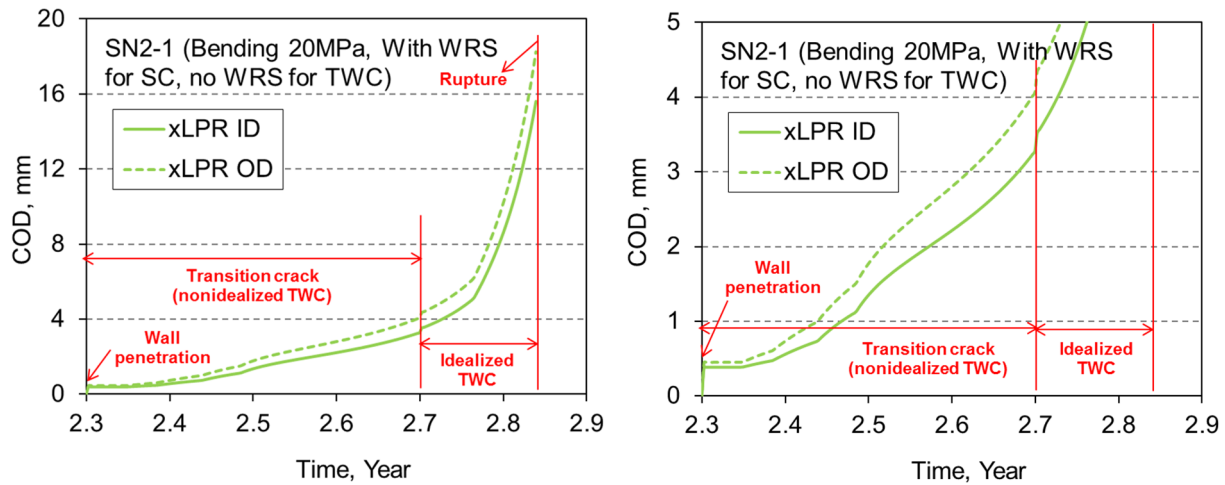
Figure 14 Stability calculation results

The COD values required for the leak rate calculations are internally calculated in xLPR using the COD module. Figure 15 shows the elastic-plastic COD values calculated up to the critical crack size. The plots on the right side are magnified views of the plots on the left side. For both cases, although the crack length was much shorter at the OD surface compared to that at the ID surface (especially immediately after wall penetration), the COD on the OD surface was larger than that at the ID surface throughout the crack growth. This behavior has been verified during the development of the crack transition model. Note that these results do not include the effect of the WRS. It is expected that the COD values will be affected by the WRS to some extent. However, by the time the critical crack size (approximately $\theta/\pi=0.5$) is reached (or even before that), the effect of the WRS will be negligible.

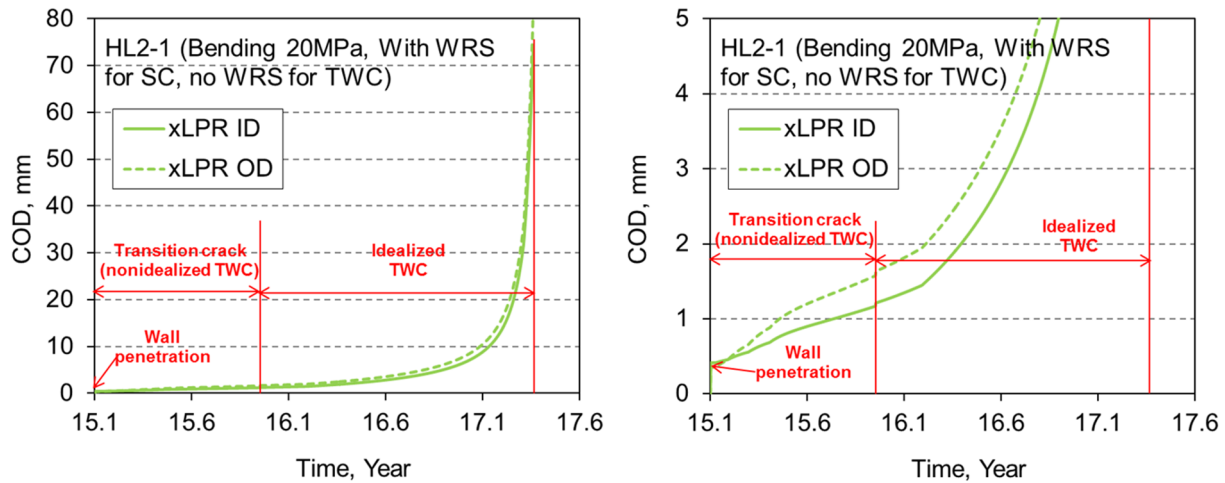
Figure 16 provides the leak rate calculation results where two calculations were conducted. The ‘GoldSim’ results are directly from the xLPR code and the ‘LEAPOR’ results are the same calculations performed outside of xLPR using a stand-alone LEAPOR code. The LEAPOR code is used within the xLPR code as a preprocessor that generates look-up tables normalized by pipe

[§] D.J. Shim, S. Kalyanam, F. Brust, G. Wilkowski, M. Smith, A. Goodfellow, “Natural Crack Growth Analyses for Circumferential and Axial PWSCC Defects in Dissimilar Metal Welds,” ASME Journal of Pressure Vessel Technology, Vol. 134(5), 051402, 2012.

and crack geometry, and loading. This requires the xLPR code to interpolate between tabulated leak rate values for geometries and loads that are not directly represented in the look-up tables. The exact interpolation methods used were developed by the Leak Rate Subgroup and is not described here for brevity. As illustrated in Figure 16, the two results show a difference in certain regions. This discrepancy is currently being reviewed by the Leak Rate Subgroup. The more important aspect of these results is the fact that the leak rate is close to 10 gpm at incipient leakage. In addition, as the crack transitions to an idealized through-wall crack and grows to the critical crack size, the leak rate values increase up to values much greater than the typical leak detection capabilities. Hence, LBB is demonstrated for both cases.

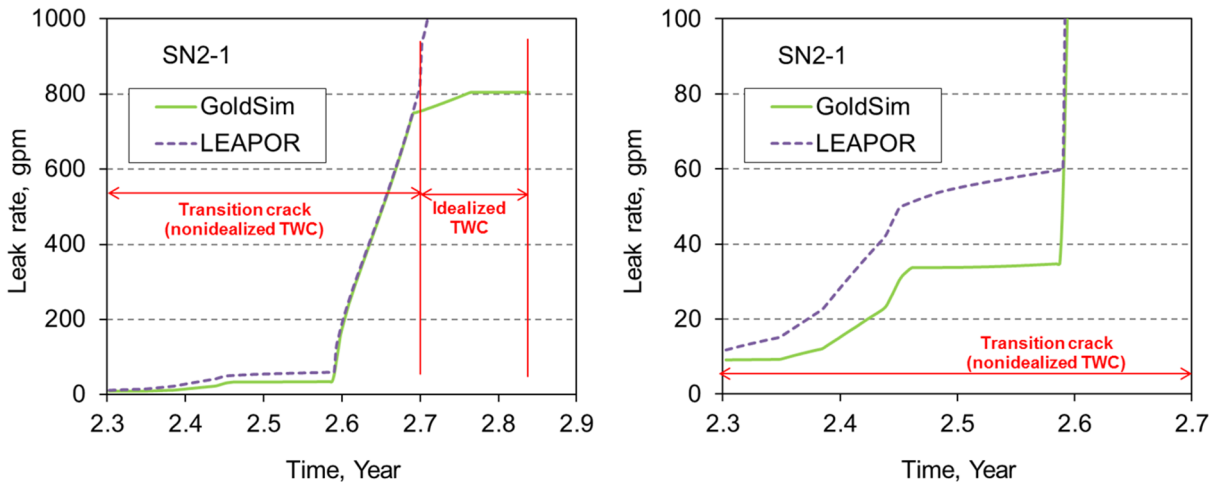


(a) Surge nozzle

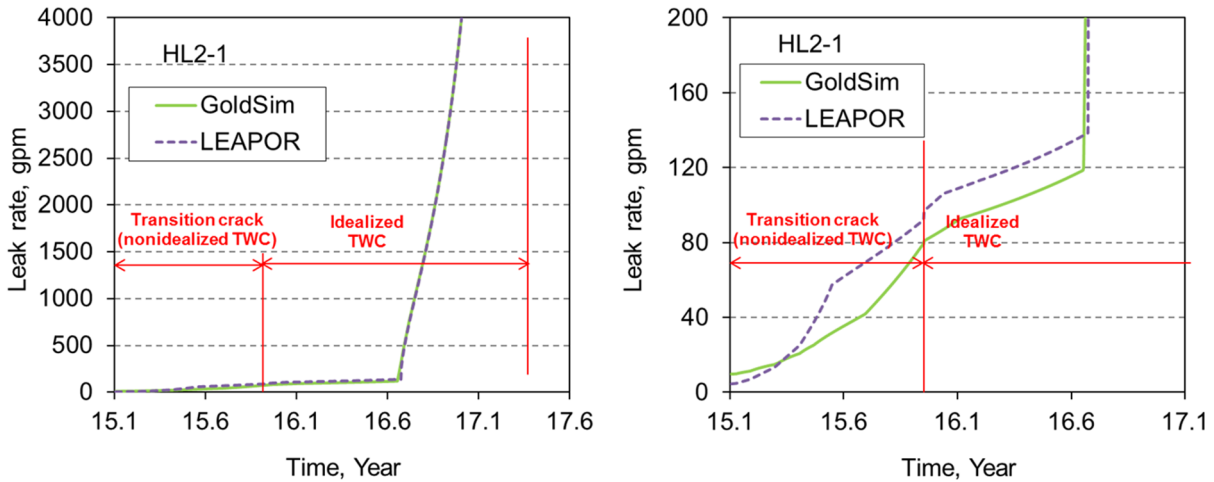


(b) Hot-leg nozzle

Figure 15 COD calculation results



(a) Surge nozzle



(b) Hot-leg nozzle

Figure 16 Leak rate calculation results

3. Conclusions

In this effort, to address the comment provided by the ERB, LBB evaluations were carried out for PWSCC in DM weld of a surge nozzle and a hot-leg nozzle. Below are the two concerns that the ERB raised.

1. Can a non-LBB situation occur for a relatively long surface crack that has been formed by a WRS that has compressive stresses in the middle of the pipe wall in combination with relatively small operating stresses from global bending? (Item 3.2)
2. Will neglecting the WRS for through-wall crack growth and COD calculation affect the LBB behavior? (Item 3.3)

To address these concerns, as recommend by the ERB, natural crack growth calculations were performed using the AFEA technique to generate a relatively long surface crack prior to wall penetration. This was done by applying an axial WRS profile with compressive stresses along with a relatively low global bending stress (20MPa). In addition, to investigate the effect of WRS on the through-wall crack growth behavior, AFEA calculations were repeated without the WRS for the through-wall crack growth portion.

As expected, relatively long surface cracks were formed from the AFEA calculations. These results were compared against the xLPR results which showed reasonable agreement. The AFEA results also demonstrated that the effect of WRS on through-wall crack growth was not significant enough to affect the LBB predictions.

The LBB analyses were conducted using the xLPR code. For both cases, the critical crack sizes were predicted to be reached after evolving to an idealized through-wall crack and the critical crack sizes were close to 50% of the circumference. In addition, the leak rates calculated for the incipient leakage were approximately 10 gpm for both cases. Although this leak rate does not include the effect of WRS on COD, the leak rates at critical crack size (or pipe rupture) are significantly greater than the typical leak detection capabilities, so the overall LBB results will not be affected by the WRS.

Note that these conclusions were drawn from limited analyses recommended by the ERB. Selection of different WRS profiles may affect the surface crack length prior to wall penetration. However, despite this variation, once the surface crack penetrates the wall thickness, the incipient leakage will be close to 10 gpm as demonstrated in the two examples above. In addition, from past work, there were no cases where a 360-degree surface crack was formed from an AFEA analysis for surge and hotleg nozzles. Based on these trends, it is suggested that the conclusions of this study are valid for different WRS profiles. If further investigation is needed, it should be approved by the xLPR Project team.